Characterisation of microparticle transport driven by ionic current conditions in electrically polarised aqueous solutions

Ryo Nagura, Kentaro Doi, Satoyuki Kawano ✉

Department of Mechanical Science and Bioengineering, Graduate School of Engineering Science, Osaka University, 1-3 Machikaneyama, Toyonaka, Osaka 560-8531, Japan
✉ *E-mail: kawano@me.es.osaka-u.ac.jp*

Published in Micro & Nano Letters; Received on 28th February 2017; Revised on 4th May 2017; Accepted on 23rd May 2017

Molecular transport technology is one of the hottest topics in micro- and nanofluidics. Target molecules are often transported by electric forces, e.g. capillary electrophoresis (EP), gel EP, biological and artificial nanopores. On the other hand, such methods are sometimes disturbed by surrounding environments because the surface effects tend to be prominent. The surface charges on the channel walls cause peculiar liquid flows in micro- and nanochannels. Thus, the isolation of electrophoretic transport from the fluidic effects is important to achieve the precise control of targets in confined spaces. In this study, a novel technique to control the transport of microparticles is proposed, where a liquid flow is involved by applying electric body forces. The direction of electrically charged microparticles is controlled by the electric forces not only on the particle but also in the liquid. Herein, an electrohydrodynamic flow is applied by preparing electrically polarised solutions. In this setup, the transport direction of particles can be changed depending on the electric forces by excessive ions, which is estimated by measuring electric conductivity.

1. Introduction: In recent, various novel phenomena in micro- and nanospaces can be experimentally discovered by using microelectromechanical systems. Molecular transport in micro- and nanofluidic channels is one of them. Especially the single molecule resolution is expected to be achieved [1]. This technology is also hoped to contribute to many research fields, such as preconcentration to improve the reactivity [2, 3], separation of molecular species [3, 4], DNA sequencer [5] and so on.

Capillary electrophoresis (EP) is often employed for single molecule analysis included in a tiny amount of working fluid without contacting. When an external electric potential is applied into the micro- and nanochannels, however, electroosmotic flow (EOF) [6, 7] is generated in the channel and sometimes interferes the molecular transport [8]. Hence, various approaches are supposed to control EOFs by changing the species of electrolyte [9], pH of the solvent [10] and by modifying the channel walls [11, 12]. On the other hand, some researchers examined to apply EOFs to suitably control the flow fields by modifying the surface charges [13] and by applying gate voltages [14, 15]. The other study reported that liquid flows in microchannels were controlled by external flow inputs by applying an additional pressure [16], whose capability might not be enough for practical use because of the excessive flow rate. Thus, developments of novel methods to control micro-scale liquid flows coupling with the external flows to manipulate transport of single molecules and microparticles.

Electrohydrodynamic (EHD) flow is also known as a technique to induce electrically-driven liquid flows in wider spaces [17, 18]. Melcher and Taylor [17] developed this principle, and experimentally [19] and theoretically [20, 21] demonstrated. EHD flows can be generated by applying Coulomb force in liquids, where the whole liquid phase has to be polarised by externally injected electrical charges. This method needs at least several tens of applied potentials to drive ion-drag liquid flows and then, the solvent is limited to non-aqueous solutions to avoid generating bubbles due to the electrolysis of water. Although many studies about micro- and nanofluidics are proposed to use aqueous solution systems, such a limitation disturb the expansion of practical applications.

In this study, we focus on the behaviour of single microparticles in electrically polarised aqueous solutions, where liquid flows are expected to be driven by ionic currents under externally applied electric potentials. The transport regime of microparticles is modified by the ion-drag flow field. Here, we propose a novel method to generate the ion-drag EHD flows [22, 23] in aqueous solution drastically decreasing the application voltage, where the external voltage does not exceed 2.0 V to avoid accelerating the electrolysis of water. We succeeded to dramatically reduce the applied voltage by preparing electrically polarised solutions. In our method, instead of charge injection, both cations and anions are separated by using an ion-exchange membrane, although the conventional methods required excessively high voltages to externally inject electrical charges into the liquids. Consequently, we succeed to observe EHD flows with the applied voltage within 2.0 V.

2. Experimental methodology: In aqueous solutions, microparticles are often electrically charged and their surfaces are partially screened by counterions which form an electric double layer (EDL). By applying an electric field, the charged particles migrate due to the electric force, so called EP and on the other hand, the EDL is known to cause a slip boundary of EOF. The directions of EP and EOF are usually opposite each other because these phenomena are governed by the opposite signs of electrical charges. Solving the Navier–Stokes equations for an incompressible liquid, the velocity of a microparticle, whose surface is electrically shielded, is represented by

$$v_{\mathrm{EP}} = \frac{2\varepsilon\zeta_{\mathrm{p}}E}{3\mu} = \frac{qE}{6\pi\mu a}, \tag{1}$$

where ε is the dielectric constant of solvent, E is the external field, ζ_{p} is the surface potential of particle, and μ is the viscosity of solvent [24]. Here is an assumption that the total amount of electrical charges is zero in the electrically neutral condition. As a result, the direction of v_{EP} is determined by E and ζ_{p}. The velocity of EOF is also expressed in the same way, taking into account surface potentials of channel walls. When the zeta potential of wall surface is given as ζ_{w} and then, the EOF velocity u_{EOF} is

© The Institution of Engineering and Technology 2017

doi: 10.1049/mnl.2017.0131

expressed as follows:

$$u_{\mathrm{EOF}} = -\frac{\varepsilon \zeta_{\mathrm{w}} E}{\mu}. \tag{2}$$

EOF is caused by highly concentrated ions in EDL and thus, the velocity profile shows plug-like flows. Assuming that electrical charges of a particle and EDL do not interact with each other, we can observe the particle velocity v_{p}, such that

$$v_{\mathrm{p}} = v_{\mathrm{EP}} + u_{\mathrm{EOF}}. \tag{3}$$

On the other hand, if the numbers of cations and anions are different in the liquid, electrical charge distributions are possibly appeared in the liquid. Under external electric fields, a liquid flow is generated by the ions that drag solvent molecules and then, the direction of flow is determined by the sign of charge carriers dominant in the liquid. In such a condition, when the electrical charges of the microparticles and excessive ions are opposite, the transport directions of the microparticle and EHD flow dragged by the dominant ions are also opposite. The relative velocity of EHD flow to that of microparticle tends to increase the force on the particle. As a result, the microparticle may be strongly dragged by the EHD flow and the direction is possibly reversed in the flow direction.

To prepare an electrically polarised solution in which electroneutrality is broken by the presence of excessive ions, we use an ion-selective diffusion between high- and low-concentration solutions divided by a cation-exchange membrane, as shown in Fig. 1. The concentrated and diluted electrolyte solutions are poured in the upper and lower channels, respectively, where diffusion of cations from the upper to the lower is enhanced. On the other hand, transport of anions are disturbed by the ion selectivity of the membrane. In this situation, the lower solution results in a cation rich condition and that is, an electrically polarised solution is achieved.

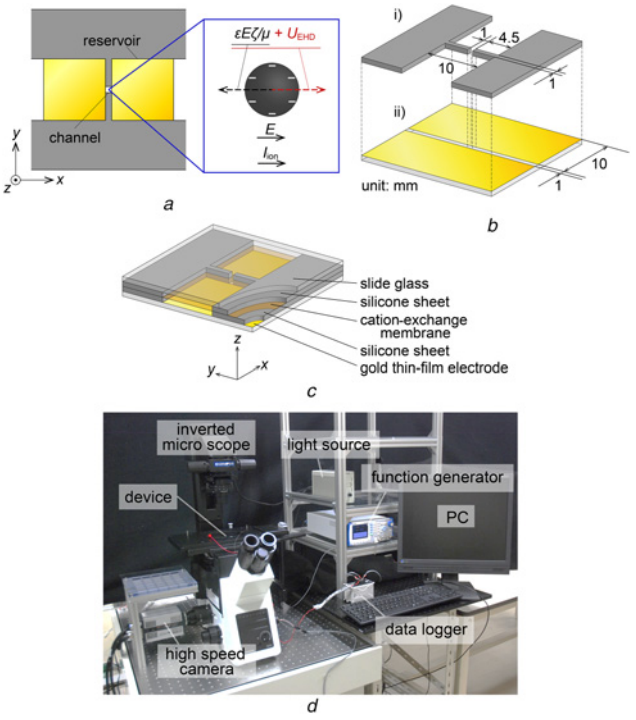

Fig. 1 *An experiment to observe the transport of electrically charged particles in an EHD flow*
a Schematic illustration of the transport mechanism of a microparticle driven by EP in EHD flow field,
b dimensions of flow channel in the experimental device,
c assembly of the multi-layered device, and
d photograph of the experimental setup

To optically observe the transport of microparticles in liquid flows in various cation concentrations, the experimental device is designed as schematically shown in Figs. 1*b* and *c*. A 127 μm thick cation-exchange membrane (Nafion®, N-115, E. I. Du Pont de Nemours and Co.) is fixed by two silicone sheets of 1 mm thick in which a flow channel and reservoirs are located, pressing them with two slide glasses from both top and bottom ends. As shown in Fig. 1*c*, the channels in the upper and lower layers are connected through the membrane in the z direction and each of them is placed between the reservoirs in the x direction. The cross-section of the channel has 1 mm width and 1 mm height, and the reservoir has 10 mm width and 1 mm height. The centre of reservoirs is aligned with the channel in the x-axis. The other end of reservoir is opened to air. The bottom surface of the lower reservoirs is covered with a thin-film Au electrode about 100 nm thick which have 10 mm width and 10 mm long. The surface area of the electrodes is 100 times larger than the cross-sectional area of the channel in order to concentrate electric field lines in the channel along the x-axis.

The mixtures of aqueous solutions poured in the upper and lower channels are shown in Tables 1 and 2. In both channels, a Tris-EDTA buffer solution (T9285, Sigma-Aldrich Co. LLC.) is used as a solvent, which can maintain the pH around eight to suppress drastic changes in the pH near the electrodes. Thus, this kind of buffer solution is conventional to treat transport phenomena of electrically charged molecules and particles. A variety of polystyrene (PSt) particles is widely used as a tracer and a 1.01 μm diameter one (Estapor®, Merck KGaA) is employed in this study. Using this size, the magnitude of Brownian motion becomes smaller than that

Table 1 Mixture of aqueous solutions in the upper and lower layers in the experimental device (Case I)

	Solution	Concentration
Case I	Upper channel	
	KCl	1.0 mol/l
	Tris-EDTA	1.0×10^{-2} mol/l
	Lower channel	
	PSt dispersion	1.0×10^{-3}%
	Tris-EDTA	1.0×10^{-2} mol/l

Table 2 Mixtures of aqueous solutions in the upper and lower layers in the experimental device (Case II–V). In Case II, in the two layers separated by the cation-exchange membrane, the electroneutral condition is maintained by the PSt particle dispersion with Tris-EDTA buffer solution in both layers. The concentration of additional KCl solution is varied in Cases III–V

	Upper & lower channels	
	Solution	Concentration
Case II	PSt dispersion	1.0×10^{-3} vol%
	Tris-EDTA	1.0×10^{-2} mol/l
Case III	PSt dispersion	1.0×10^{-3} vol%
	Tris-EDTA	1.0×10^{-2} mol/l
	KCl	1.0 mol/l
Case IV	PSt dispersion	1.0×10^{-3} vol%
	Tris-EDTA	1.0×10^{-2} mol/l
	KCl	1.0×10^{-1} mol/l
Case V	PSt dispersion	1.0×10^{-3} vol%
	Tris-EDTA	1.0×10^{-2} mol/l
	KCl	1.0×10^{-2} mol/l

© The Institution of Engineering and Technology 2017

of the electric forces. PSt particles are known to be negatively charged in the solutions of pH 8 and thus, they are expected to respond to the opposite direction of externally applied electric fields. Here, as a first step, we employ the conventional tracer particle without any treatment except for maintaining pH in the buffer solution, although charge neutral particles are preferable to trace the behaviour in liquid flows driven by electric forces. Unfortunately, some kinds of preferable tracer whose density is near water are usually negatively charged in polar solvents [25–28]. As shown in Table 1, a KCl solution and PSt dispersion are poured in the upper and lower solutions, respectively. Hereafter, this condition is called as Case I. In this situation, K^+ ions are expected to diffuse into the lower layer according to the concentration difference between the two layers. On the other hand, the transport of Cl^- ions is filtered by the cation-exchange membrane. When the external electric field is applied into the lower channel, as excessive K^+ ions drag the surrounding solvent molecules, a body force is induced in the liquid in terms of fluid mechanics. In such a condition, the transport of a PSt particle is affected by surrounding flows as well as its own electrophoretic transport and consequently, the velocity of the particle is determined by the superposition of the competitive forces.

To compare the cation rich solution with the electrically neutral one, we also carry out another experiment using an electrically neutral solution. In Table 2, the same PSt dispersion with Tris-EDTA buffer is poured in both channels. Hereafter, we call this condition as Case II. In the solutions listed in Table 2, diffusions of ions via the cation-exchange membrane are not observed because of the same concentrations between the two layers. The solutions are equilibrated at electroneutral conditions. When external electric fields are applied in the lower channel, PSt particles are expected to respond to the applied fields by its electrophoretic transport. On the other hand, the presence of both positive and negative ions suppresses the induction of anisotropic electric body forces in the liquid because of the attractive Coulomb force between the two species.

In order to discuss the effect of excessive K^+ ions in the lower channel on the liquid flows, the conductance of ionic currents is measured at first. If the diffusion of K^+ ions passing through the cation-exchange membrane breakdowns the electronuetrality, the difference in the lower solution between Cases I and II will be observed. In Case I, K^+ ions dominantly act as charge carriers to generate an ionic current and on the other hand, in the other cases, both K^+ and Cl^- ions can contribute to the ionic current. Varying the applied voltage, we can also recognise the difference in the current-voltage characteristics between them. In addition, measuring the characteristics for various KCl concentrations such as Cases III–V, the unique property of the cation rich solution is clearly characterised.

Using the experimental setup as shown in Fig. 1*d*, the thin-film Au electrodes in the lower reservoirs are connected to a function generator (WF1973, NF Corp.) to apply electric potentials and an ammeter with data logger (NR-500, Keyence Corp.), where an electrode at the negative side along the x-axis is at high potential. The current-voltage characteristics of solutions are measured by this system with the sampling rate of 1 ms. Optical observation is carried out by the high speed CMOS camera (Zyla sCMOS, Andor Co., Ltd.) connected to the inverted microscope (IX73, Olympus Corp.), where the window size is 2560×500 ($x \times y$) pixels with the spatial resolution of 0.11 μm and the frame rate is 40 fps. The velocity of microparticles is extracted and analysed by the single particle tracking method.

3. Results and discussion: In a preliminary experiment, we estimated the ion diffusion process passing through a cation-exchange membrane by monitoring the potential difference between the upper and lower reservoirs. The potential difference between both ends across the membrane was measured by using Au wire probes, which were connected to a digital multimeter (DME1600, Kikusui Electronics Corp.). Sampling rate was once every 10 min, and the duration of the measurement was 24 h. As a result, the potential difference was reached a steady state about 18 h after injecting the solutions. Although the detailed distribution of cations has not yet been clarified, the electric conductance of ionic current was evaluated in comparison between electroneutral and electrically charged solutions. In the result shown in Fig. 2, the slope of the potential difference decreased as time passed and the transition was almost converged after 12 h as shown in the inset of Fig. 2. This behaviour was caused by the diffusion of cations crossing the membrane. At the steady state, ion distributions were equilibrated as a result of competitive transport between the diffusion and EP. Such a potential difference at the equilibrium is known as the membrane potential. Although the Au probes did not react with electrolyte ions and therefore, might not be available to quantitatively sense ion distributions, they were effective to roughly detect the transition of environments. It was suggested that we could estimate whether the ion transport was equilibrated or not by measuring the time evolution of the potential difference. To investigate the transport of microparticles in a stable liquid phase that was electrically polarised, the solutions had to be settled at equilibrium conditions before observations. Therefore, injecting the solutions into the reservoirs, we needed to wait for 18 h before starting measurements using the experimental device.

The steady currents in the solution of Cases I and II were measured in the range from 0.5 to 2.0 V of applied voltages. The result of current-voltage characteristics is shown in Fig. 3. At the applied voltage lower than 1.0 V, there was no meaning currents in both electroneutral and cation rich conditions. When an electric

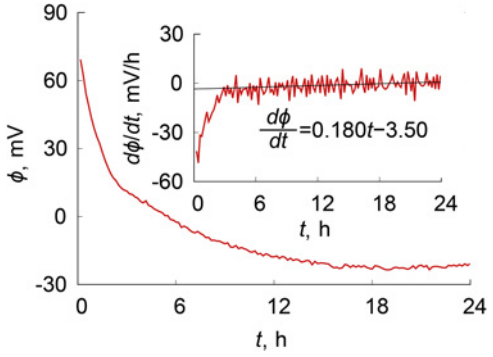

Fig. 2 *Time evolution of potential difference ϕ between the upper and lower reservoirs. The time derivative of ϕ is also shown in the inset, where the black solid line is resulting from the linear least square fit for the data between t = 12 and 24 h*

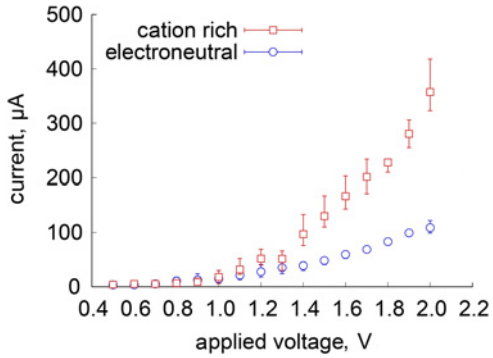

Fig. 3 *Current-voltage characteristics resulting from cation rich and electroneutral solutions, where red squares for experimental data from the cation rich solution of Case I and blue circles for data from the electroneutral solution of Case II. Error bars show the range from the minimum to maximum values*

© The Institution of Engineering and Technology 2017

doi: 10.1049/mnl.2017.0131

potential was applied into the liquids, electrolyte ions were attracted to the electrode and formed EDL on the electrode surfaces. Although such an unsteady ion transport, so called non-Faradaic current, could be observed within a short period, it immediately converged to an equilibrium condition. To generate steady current states, electrolyte ions have to transport constantly in the solution, exchanging electrical charges by electrochemical reactions at the electrode surfaces. This is a reason why steady currents could not be observed lower than 1.0 V, where effective electrochemical reactions did not occur. On the other hand, steady currents tended to increase over 1.0 V in both solutions. In this level, the electrolysis of water was observed because of the ideal electrochemical potential of 1.23 V. We have not clarified detailed effects of water electrolysis on local heat transfer near the electrode surfaces. Therefore, the applied voltage and measurement time were limited by a stable condition in which hydrogen and oxygen bubbles could not be observed at the electrodes. Each data point in Fig. 3 shows the average of four time trials. As a result, the magnitude of steady current in Case I is three times larger than that of Case II. This difference emphasises an increase in electric conductivity in the cation rich condition. This experimental result suggested that the transport of K^+ ions from the upper to the lower layer passing through the Nafion membrane actually contributed to improve the conductivity. Furthermore, the drastic increase of the conductivity was possibly attributed to the presence of protons, because the conductivity of proton was approximately one order of magnitude larger than that of K^+, and protons captured in the membrane possibly replaced by K^+ ions in part. Direct measurement methods of ion concentrations are also required to be improved in our future study.

For comparison, steady currents in the solutions of Cases III–V were also measured in the range from 0.5 to 2.0 V of the applied voltage. The result of current-voltage characteristics is shown in Fig. 4. Each data point consists of four time trials. In the same manner as Fig. 3, steady currents were apparently observed over 1.0 V of the applied voltage in each case. The magnitude of the steady current increases with increasing the salt concentrations. These results are also explained by the improvement of ion conductivity, involving the transport of Cl^- ions as well as K^+ ions. Both species have a role of supporting electrolytes to maintain the high conductivity in the whole space of the solution. In Cases II and V, both solutions contain Tris-EDTA buffer, which also acts as a charge carrier to maintain a constant pH. The concentration of KCl in Case V is low and comparable with Tris-EDTA buffer. In such a case, KCl may not sufficiently work as a good supporting electrolytes in the steady current conditions. The concentrations of electrolytes are on the same order in Cases II and V and a little differences are within the measurement error range. An

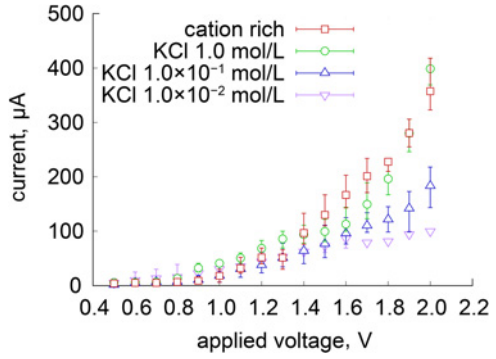

Fig. 4 *Current-voltage characteristics of cation rich and electroneutral solutions for a variety of concentrations of KCl, where red squares for cation rich solution of Case I (same as in Fig. 3), green circles, blue triangles, and purple inverted triangles for KCl solutions with 1.0 mol/l (Case III), 1.0×10^{-1} mol/l (Case IV), and 1.0×10^{-2} mol/l (Case V), respectively. Error bars show the range from the minimum to maximum values*

interesting point is that the current-voltage curve obtained by the cation rich solution was placed between that of 1.0 mol/l and 1.0×10^{-1} mol/l of KCl solutions and thus, the conductivity of the cation rich solution was on the same order of 1.0×10^{-1} mol/l one. The conductivity of ionic current is proportional to the concentration, assuming uniform ion distributions. The excess K^+ ions and protons contributed to the conductivity as electrical charges, where the absence of counterions of Cl^- might cause to increase the conductivity of cations, reducing constraints of the attractive force by Coulomb interactions.

The *x* component of terminal velocity of a PSt particle is shown in Fig. 5 ranging from 0.5 to 2.0 V of the applied voltages. The electrically charged PSt particle was confirmed to move along the *x*-axis when an electric field was applied in the *x* direction. To overview the relationship between the transport velocity and the ionic current, current-voltage characteristics are also shown in the same figure. The results shown in Figs. 5*a* and *b* correspond to electroneutral and cation rich conditions, respectively. In Fig. 5*a*, the terminal velocity was observed only if the external voltage was applied over 1.0 V. This voltage value corresponded to the lower limit at which a steady current could be observed. Under the limit, electric

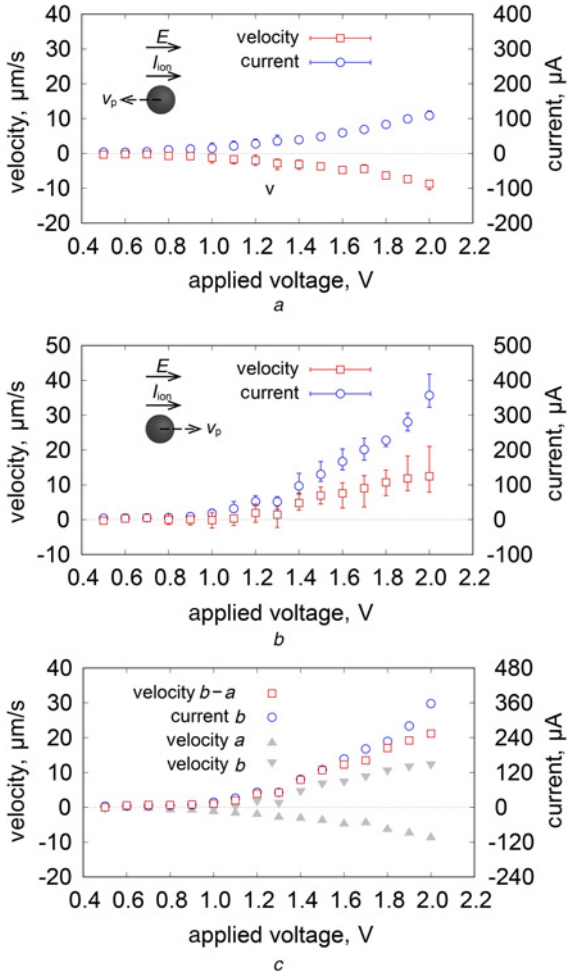

Fig. 5 *Transport velocities of a PSt particle associated with the current-voltage characteristics in*
a electroneutral solution of Case II and,
b cation rich solution of Case I, where red squares present the terminal velocity with the left axis and blue circles the steady current with the right axis;
c The difference of velocities between (a) and (b) with the left-axis, where the velocities in (a) and (b) and the current of (b) with the right-axis are also shown in the same figure. Error bars indicate the range from the minimum to maximum errors

© The Institution of Engineering and Technology 2017

fields was not affected deeply in the solution because the electrode surfaces were shielded by EDL. In other words, the transport of particles was not recognised without ionic current in the solution. The steady currents guaranteed the presence of electric fields to drive electrolyte ions. With ionic currents, the particle moved to the positive electrode in the negative x direction. PSt particles were negatively charged in the Tris-EDTA buffer solution and responded in the opposite direction to the external electric field. As the applied voltage increased, the transport speed also increased. This negative velocity was resulted from the electrophoretic transport of the microparticle. In this case, the ionic current was generated by the electrolysis of water at the electrode surfaces and assisted by the transport of both K^+ and Cl^- ions in the solution. Due to the presence of both ion species whose transport numbers were almost the same, any electric body force was not be applied to induce liquid flows. As shown in Fig. 5*b*, the terminal velocity was also observed only when the external voltage over 1.0 V was applied in the cation rich solution corresponding to Case I. As previously discussed, the ionic current consisted of both electrolysis of water and transport of electrolyte ions, although cations were more excessive than anions. Therefore, under the limit of 1.0 V, meaningful currents could not be observed due to shielding of the electrode surfaces by EDL. On the other hand, when we applied the voltage over 1.0 V, a negatively charged PSt particle moved to the positive direction in the x-axis toward the negative electrodes. This result seems to be physically contradicted without considering the effect of flow fields, because the negative charge actively transports to the negative electrode. This phenomenon is explained by considering a liquid flow which is electrically induced in the channel. By the existence of excessive cations confirmed in Fig. 3, we could figure out that this reverse response was caused by an EHD flow generated in the channel. The flow channel was opened to air at both ends and the solution maintained the surface meniscus. It was confirmed that the EHD flow was not observed in the upper layer, but limited in the lower channel. In such a condition, it is possible to induce the liquid flows only in the positive x direction satisfying mass conservative law. Based on the transport velocity of a microparticle in electroneutral conditions introduced by (3), that in an almost uniform flow field is possibly expressed as

$$v_p = v_{EP} + u_{EHD}, \tag{4}$$

where u_{EHD} is caused by additionally increased ion concentrations and is driven by the electric body force. In this situation, the transport of a microparticle driven by EP is in an EHD flow. Depending on the magnitude of u_{EHD}, the transport direction of particle can be reversed.

We previously measured the electrical charge of a 1.0 μm diameter PSt particle exposed to ac electric fields in pure water. As a result, we obtained the surface charge density of $\sigma = 42\,\mu C/m^2$. Using this value, the effect of electroosmosis could be evaluated. Here, we assumed that the applied electric field in a 1.0 mm length channel was uniformly 2.0×10^3 V/m and that the EOF was a plug flow. For the particle velocity of $v_p = -9\,\mu m/s$ at the applied voltage of 2.0 V as shown in Fig. 5*a*, the velocity of EOF resulted in $u_{EOF} = 19\,\mu m/s$ from (3), taking into account the electrophoretic velocity estimated by (1) as $v_{EP} = -28\,\mu m/s$. As shown in Fig. 5*c*, the difference in the particle velocity between Figs. 5*a* and *b* represented the flow velocity caused by additionally increased cations, such that $\Delta u = u_{EHD} - u_{EOF}$. Δu was also estimated and for example, we obtained $\Delta u = 21\,\mu m/s$ for an applied electric potential of 2.0 V. It was found that the flow velocity clearly correlated with the characteristics of ionic current.

Snapshots of PSt particles observed in the experiments are shown in Fig. 6. As shown in Fig. 6*a*, it was found that the particles transport with a constant velocity along the x-axis in the electroneutral

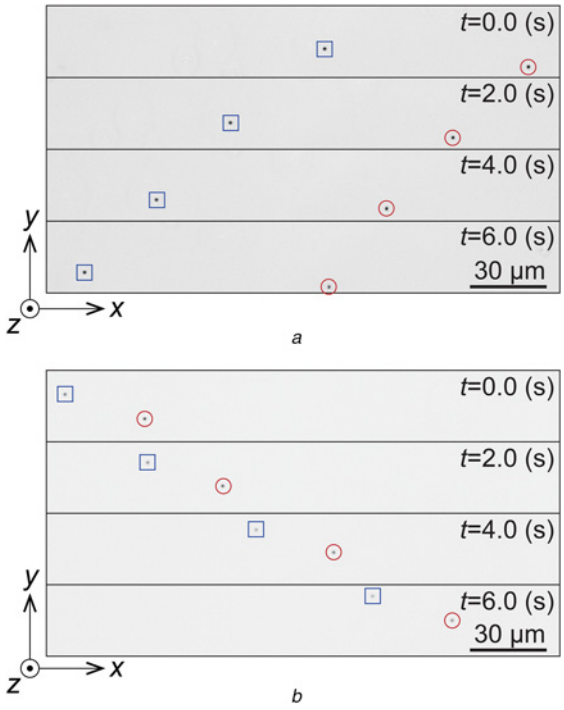

Fig. 6 *Snapshots of translocated PSt particles observed at t = 2.0, 4.0, and 6.0 s after applying an electric voltage of 2.0 V in*
a Electroneutral solution of Case II and,
b Cation rich solution of Case I, where the ionic current is directed to the positive direction of x-axis. Two particles are marked by open square and open circle

condition, corresponding to the case of Fig. 5*a*. As mentioned previously, the particles were driven by EP of their own electrical charges and the transport direction was opposite to the ionic current. On the other hand, in a cation rich condition as shown in Fig. 6*b*, PSt particles moved in the reverse direction to that in Fig. 6*a* because an EHD flow strongly dragged the particles. Consequently, the particles were transported with the constant velocity in the same direction of the ionic current. Using the present experimental device, we could succeed to observe an EHD flow induced by cation transport. We also continue to improve our device to clearly generate the cation-induced flows reducing the complexities.

In this study, at first, we focused on cation driven liquid flows separated by a Nafion membrane. On the other hand, Ag/AgCl electrodes are also a preferable candidate to apply electric potentials with steady currents, in which Cl^- ions have a role of main carrier. Anion driven flows generated by using anion-exchange membrane are also in our interests and are the next step.

4. Conclusion: In this study, we have succeeded to observe an EHD flow in aqueous solution by generating electrically charged solution. This solution was realised by cation selective diffusion passing through the cation-exchange membrane. We measured the current-voltage characteristics of the solutions and confirmed that a cation rich condition was achieved in the concentration of 1.0×10^{-1} mol/l. In the traditional understanding, electrically charged solution in bulk is unstable in nature. Thus, this result disprove the past common view. Furthermore, when an external electric field is applied into the solution, we have also confirmed that an EHD flow is generated within 2.0 V of applied voltages by considering particle response. Therefore, this study can expand the applicable field of knowledge about EHD flows and related technologies. In addition, it is important that the terminal velocity was on the order of 10 μm/s. When considering to control the

© The Institution of Engineering and Technology 2017

doi: 10.1049/mnl.2017.0131

flow in microspaces, this study can contribute to improve the accuracy. If the flow control with the resolution of 10 μm/s is attained, further developments of micro- and nanofluidic devices are expected. Although salt concentrations and pH are actually critical parameters in biological applications, our prototype system is possibly improved for flow control techniques in biological devices, optimising the structure, ion species and concentrations. The development of measurement methods of individual ion species is an important issue. These subjects will be featured in our next project.

5. Acknowledgments: This study was supported by Japan Society for the Promotion of Science, Grants-in-Aid for Scientific Research (JSPS KAKENHI) grant no. JP16H06504 in Scientific Research on Innovative Areas 'Nano-Material Optical-Manipulation'.

6 References

[1] Hanasaki I., Nagura R., Kawano S.: 'Coarse-grained picture of Brownian motion in water: role of size and interaction distance range on the nature of randomness', *J. Chem. Phys.*, 2015, **142**, pp. 104301–1–104301-11

[2] Wang Y.-C., Han J.: 'Pre-binding dynamic range and sensitivity enhancement for immuno-sensors using nanofluidic preconcentrator', *Lab Chip*, 2008, **8**, pp. 392–394

[3] Song H., Wang Y., Garson C., *ET AL.*: 'Nafion-film-based micro-nanofluidic device dor concurrent DNA preconcentration and separation in free solution', *Microfluid. Nanofluid.*, 2014, **17**, pp. 693–699

[4] Meacher R.J., Won J.-I., McCormick L.C., *ET AL.*: 'End-labeled free solution electrophoresis of DNA', *Electrophoresis*, 2005, **26**, pp. 331–350

[5] Tsutsui M., Taniguchi M., Yokota K., *ET AL.*: 'Identifying single nucleotides by tunnelling current', *Nat. Nanotech.*, 2010, **5**, pp. 286–290

[6] Daiguji H., Yang P., Majumdar A.: 'Ion transport in nanofluidic channels', *Nano Lett.*, 2004, **4**, pp. 137–142

[7] Schoch R.B., Han J., Renaud P.: 'Transport phenomena in nanofluidics', *Rev. Mod. Phys.*, 2008, **80**, pp. 839–883

[8] Wang W., Zhou F., Zhao L., *ET AL.*: 'Measurement of electroosmotic flow in capillary and microchip electrophoresis', *J. Chromatogr. A*, 2007, **1170**, pp. 1–8

[9] Mendes A., Branco L.C., Morais C., *ET AL.*: 'Electroosmotic flow modulation in capillary electrophoresis by organic cations from ionic liquids', *Electrophoresis*, 2012, **33**, pp. 1182–1190

[10] Masselter S.M., Zemann A.J.: 'Influence of buffer electrolyte pH on the migration behavior of phenolic compounds in co-electroosmotic capillary electrophoresis', *J. Chromatogr. A*, 1995, **693**, pp. 359–365

[11] Liu Y., Fanguy J.C., Bledsoe J.M., *ET AL.*: 'Dynamic coating using polyelectrolyte multilayers for chemical control of electroosmotic flow in capillary electrophoresis microchips', *Anal. Chem.*, 2000, **72**, pp. 5939–5944

[12] Sola L., Chiari M.: 'Modulation of electroosmotic flow in capillary electrophoresis using functional polymer coatings', *J. Chromatogr. A*, 2012, **1270**, pp. 324–329

[13] He Y., Tsutusi M., Fan C., *ET AL.*: 'Controlling DNA translocation through gate modulation of nanopore wall surface charges', *ACS Nano*, 2011, **5**, pp. 5509–5518

[14] Guan W., Reed M.A.: 'Electric field modulation of the membrane potential in solid-stateion channels', *Nano Lett.*, 2012, **12**, pp. 6441–6447

[15] He Y., Tsutusi M., Fan C., *ET AL.*: 'Gate manipulation of DNA capture into nanopores', *ACS Nano*, 2011, **5**, pp. 8391–8397

[16] Fütterer C., Minc N., Bormuth V., *ET AL.*: 'Injection and flow control system for microchannels', *Lab Chip*, 2004, **4**, pp. 351–356

[17] Melcher J.R., Taylor G.I.: 'Electrohydrodynamics: a review of the role of interfacial shear stresses', *Annu. Rev. Fluid Mech.*, 1969, **1**, pp. 111–146

[18] Saville D.A.: 'Electrohydrodynamics: the Taylor-Melcher leaky dielectric model', *Annu. Rev. Fluid Mech.*, 1997, **29**, pp. 27–64

[19] Trau M., Saville D.A., Aksay I.A.: 'Assembly of colloidal crystals at electrode interfaces', *Langumuir*, 1997, **13**, pp. 6375–6381

[20] Ristenpart W.D., Aksay I.A., Saville D.A.: 'Assembly of colloidal aggregates by electrohydrodynamic flow: kinetic experiments and scaling analysis', *Phys. Rev. E*, 2004, **69**, pp. 021405-1–021405-8

[21] Ristenpart W.D., Aksay I.A., Saville D.A.: 'Electrohydrodynamic flow around a colloidal particle near an electrode with an oscillating potential', *J. Fluid Mech.*, 2007, **575**, pp. 83–109

[22] Doi K., Yano A., Kawano S.: 'Electrohydrodynamic flow through a 1 mm^2 cross-section pore placed in an ion-exchange membrane', *J. Phys. Chem. B*, 2015, **119**, pp. 228–237

[23] Yano A., Doi K., Kawano S.: 'Observation of electrohydrodynamic flow through a pore in ion-exchange membrane', *Int. J. Chem. Eng. Appl.*, 2015, **6**, pp. 254–257

[24] Henry D.C.: 'The cataphoresis of suspended particles. part I- the equation of caraphoresis', *Proc. R. Soc. London, Ser. A*, 1931, **133**, pp. 106–129

[25] Midmore B.R., Hunter R.J.: 'The effect of electrolyte concentration and co-ion type on the potential of polystyrene latices', *J. Coll. Interface Sci.*, 1988, **122**, pp. 521–529

[26] Mangelsdorf C.S., White L.R.: 'Effects of stern-layer conductance on electrokinetic transport properties of colloidal particles', *J. Chem. Soc. Faraday Trans.*, 1990, **86**, pp. 2859–2870

[27] Kirby B.J., Hasselbrink E.F.Jr.: 'Zeta potential of microfluidic substrates: 1. Theory, experimental techniques, and effects on separations', *Electrophoresis*, 2004, **25**, pp. 187–202

[28] Kirby B.J., Hasselbrink E.F.Jr.: 'Zeta potential of microfluidic substrates: 2. Data for polymers', *Electrophoresis*, 2004, **25**, pp. 203–213

© The Institution of Engineering and Technology 2017